Science of Sintering, **55** (2023) 71-80

https://doi.org/10.2298/SOS2301071M

UDK: 666.647; 675.017.5

Deterioration Characterization during Thermal Shock Testing

Sanja Martinović[1], MilicaVlahović[1], Tatjana Volkov Husović[2*)]
[1]University of Belgrade, Institute of Chemistry, Technology and Metallurgy, 12 Njegoševa St., 11000 Belgrade, Serbia
[2]The University of Belgrade, Faculty of Technology and Metallurgy, Karnegijeva 4, 11070 Belgrade, Serbia

Abstract:

Thermal shock stability plays a great role in the selection of optimal refractory material. Different methods of characterization were developed for this purpose, including the implementation of nondestructive testing. Image analysis is a very well method for characterization of different materials structures, as well as changes and occurred defects in structure caused by different influences. In this paper, possible application of image analysis will be presented related to the monitoring thermal shock behavior of selected refractory materials. Different parameters such are R parameter, level of destruction, as well as determination of morphological descriptors (area, perimeter, diameter, roundness) using Image analysis, will be presented.

Keywords*: Thermal shock; Refractories; R parameters. Image analysis.*

1. Introduction

The thermal shock behaviors of ceramic, especially refractory materials is very important and have a great influence on materials selection and application [1-6]. Many different techniques, tests and approaches were developed for thermal shock behavior characterization. Some of the methods are experimental and standardized [7,8], while others are based on the prediction of sample behavior based on principles of materials characteristics [9-12] and/or heat transfer conditions [13-20]. Standard tests include visual inspection of the sample during testing, which could not be sufficient for material characterization and life–time prediction. The first attempt to overcome this problem was to develop prediction methods that use R parameters [13-20] and/or temperature differences [4,21-22]. R parameters are divided into fracture resistance parameters (R and R') and damage resistance parameters (R''' and R'''') [15-20]. Usual equations for describing R parameters are given in Table I.

The first group of parameters, called fracture resistance parameters, is most suitable for use with brittle materials without microspores and micro cracks (R and R'). Calculation of these parameters is based on the thermo-mechanical properties of the material that have an impact on the formation of cracks due to thermal stress. The second group of parameters, named damage resistance parameters, is more suitable for ceramic materials with microspores and micro cracks (R''' and R'''') while their calculation is based on the material properties that affect the growth of crack and resistance to its expansion during the thermal shock. R_{st} is a crack stability parameter that is proportional to the critical temperature for crack propagation.

*) **Corresponding author:** tatjana@tmf.bg.ac.rs

All parameters can be calculated from the measured values of thermo-mechanical properties. It is well known that the cracks created during thermal shock testing are the result of a mismatch of thermal expansion between different phases thus inducing stress in the material. More precisely, the difference in the thermal expansion of the different phases creates large tensile stress around the particles of the individual phases, which causes the formation of many micro cracks, and thence a large decrease of strength and modulus of elasticity [13-20]. The equations based on R parameters do not take into account the heat transfer, which also has a large impact on material behavior. This deficiency is partly bridged by the use of some equations for temperature differences.

During the sudden cooling of the heated sample, the thermal stresses are generated that are tensile at the surface and compressive at the center of the sample. If this stress is large enough to be almost equal to fracture strength, cracks and defects can occur in the material structure.

Tab. I Resistance parameters [13-20].

Resistance factor	Equation	Number of Eq.
First fracture parameter	$R = \sigma \frac{(1-\nu)}{E\,\alpha}$	(1)
Second fracture parameter	R' = k R	(2)
First damage parameter	$R''' = \frac{E}{\sigma^2(1-\nu)}$	(3)
Second damage parameter	$R'''' = \frac{\gamma_{wof} \cdot E}{\sigma^2}$	(4)
Damage parameter	$R_{st} = \sqrt{\frac{\gamma_{wof}}{E \cdot \alpha^2}}$	(5)

Where E is Young's modulus, σ is fracture stress, α is the thermal expansion coefficient, υ is Poisson ratio, k is the thermal conductivity, and γ_{wof} is the work of fracture.

Evaluating the material according to their resistance to sudden temperature changes is based on the perceived critical temperature difference (ΔT_c) needed to cause a substantial strength degradation of the sample during heating or cooling. In this way, the maximum stress that occurs at the surface after a sudden temperature change can be determined Eq. (6), where the defined ΔT_c depends not only on heat transfer conditions but also on the mechanical material properties. Also, various analyzes show that sample geometry and/or dimensions have a significant impact on thermal stress caused by cooling or heating since the Biot number is, among the other values, proportional to the characteristic dimension (distinctive length, a) (Bi = ah/k) in Eq. (6) [21-23].

Critical temperature difference (ΔT_c) value can also be defined through the relevant thermal and mechanical properties of samples, according to Eq. (7), where 1 indicates properties of the material (sample subjected to testing) while 2 designate the properties of fluid used for cooling during testing.

Critical values of the temperature difference (ΔT_c) in the function of the Biot number is given by an Eq. (6) [1-2,21-23]. The expression that link surface stress and Biot's number, for cases of low Biot values is as follows:

$$\frac{1}{\sigma_{max}} \approx \frac{A}{B_i} \qquad (6)$$

Where A is the coefficient, with values presented in the literature, and depending on the author are A=4 (Bradshaw), A=3 (Chang) and A=3.25 (Manson) [17,20].

The temperature difference representing the sensitivity of the material to the thermal shock can also be shown by Eq. (7) [13,20]:

$$\Delta T = \left(\frac{\sigma k}{E\alpha}\right)\left(\frac{a}{h}\right) \quad (7)$$

In the case that existed conditions of heat transfer induce the occurrence of long cracks, then the equation proposed by Hasselman is usually used, presented as Eq. (8) [3,5]:

$$\Delta T = \left(\frac{k}{\alpha}\right)\left(\frac{\gamma}{E}\right)^{\frac{1}{2}}\left(\frac{a}{h}\right) \quad (8)$$

The maximum temperature difference that the material can be exposed without the damage occurring is also used as a measure of the sensitivity of the material to the thermal shock. The equation used to define the maximum temperature difference that the material withstands is usually used in the form of an Eq. (9) [21-24].

$$(\Delta T)_{max} = \left[1{,}451\ \frac{\sigma\ (1-\nu)}{E\alpha}\right]\left[1 + 6{,}82\ \left(\frac{k}{hd}\right)\right] \quad (9)$$

Another attempt to evaluate the thermal stability of material was to use a non–destructive method such as ultrasonic characterization of material under exposure to thermal shock thus providing the possibility of monitoring cracks formation and growth based on the changes in ultrasound propagation velocity [23-25]. Also some papers were interesting on sintering conditions and sintering temperature rate on mechanical and thermal properties in general [26, 27]. Besides that, the development of digital cameras as well as digital photographs, well known as images enable another approach and the development of a variety of programs for further image analysis [28-31]. This paper is occupied with some possibilities of using image analysis for the determination morphology of defects that occurred in the sample during thermal shock testing.

2. Materials and Experimental Procedures

Results presented in this paper are related to the alumina based low cement castables. Preparation of samples was usual for this type of castables and explained in detail in previous papers [33,34]. For the achievement of better properties related to refractory application, samples were sintered at different temperatures (1100, 1300, and 1600°C), with a detailed analysis of influence of the sintering temperature on the thermal and mechanical properties, as well as thermal stability. Water quench test as standard experimental procedure was applied for thermal stability testing [40]. Thermal and mechanical properties are investigated and results were published in detail [33,34].
Image of the samples was monitored using digital image in order to continue with image analysis. Samples were cubes, with 4 cm length. For the better statistical analysis, all sides were monitored (five for analysis, and one for marking), and at the Fig. 1. characteristic images before testing, and after 40 cycles are given for different sintering temperatures. Images presented at the Fig. 1. were obtained using Image analysis program [32] for highlitning observed damages with red coclor, which is convinient for further image analysis.

2.1. Image analysis principals

Image analysis is a specific tool used to determine different parameters, valuable for materials characterization; such are grain size, damaged surface, ratio of a component, length and diameter of fiber, shape of micro constitution or phase, fracture detection and measurement of the fracture length. All of these parameters are closely related to the

characteristics of the investigated material and behavior in specific conditions of thermal shock [37-39]. In this paper, possibilities of using image analysis for defects characterization will be presented.

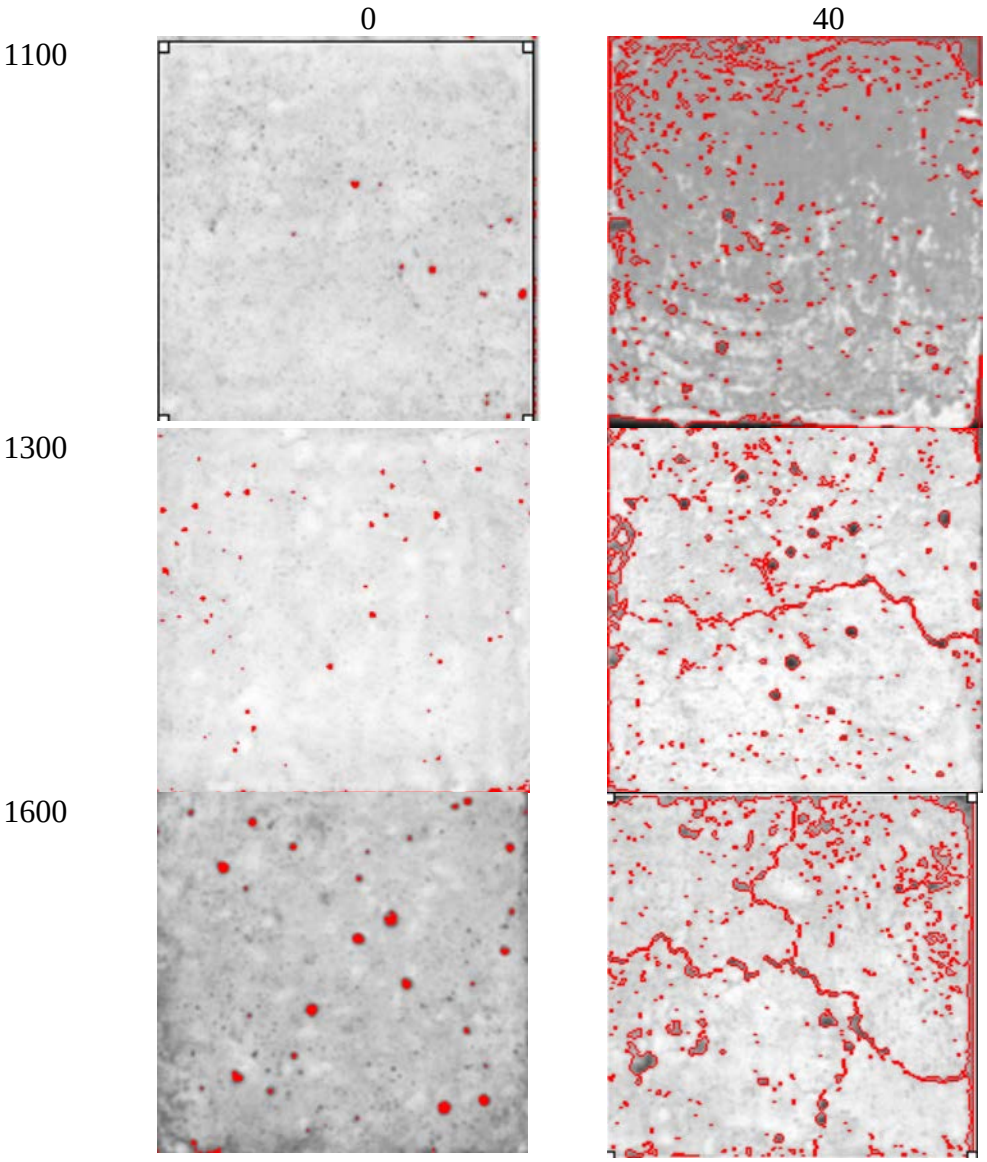

Fig. 1. Image of the sample using OM [30-36, 40] (length 4 cm).

2.2. Defects characterization: number and area of defects and level of degradation

Thermal shock causes spalling and defects during the time of testing that is cycles of heating and cooling. However, standard available testing methods [7-8,42] do not offer quantification of the damaged area of sample surface. Using some of the existing image analysis procedures, surface characterization including defects examine via their number and area, as well as total destructed area, allowed to calculate level of degradation [34,35].

2.3. Morphological analysis of defects–morphological descriptors

Besides valuable information from defects characterization (number and area defects, level of degradation) which can be used for the estimation of the material lifetime, a more detailed study can be achieved by the analysis of the morphological parameters regarding defects. Usual descriptors used for image analysis could be: area, diameter (max, min, mean), radius (max, min, mean), perimeter, fractal dimension, roundness and other [30].

2.4. Resistance parameters

In this paper two different R parameters were chosen to represent thermal stability of samples, fracture R' and damage R‴ resistance parameters. These parameters were calculated based on the strength degradation and other mechanical characteristics of samples for all sintering temperatures.

3. Results and Discussion

3.1 Defects characterization: number and area of defects and level of degradation

Surface characterization during thermal stability testing can be achieved using image analysis through determining the defects number and area as well as the total area of degradation:

$$P_i = \frac{P}{P_0} \cdot 100\% \qquad (10)$$

Where P_i is the level of degradation after *i* cycles, P is the total degradation area after the certain thermal shock cycles number, P_0 is the initial surface area before testing.
The level of degradation (P_i) is a significant parameter with reliable quantification of degradation compared to visual inspection, as is noted in some standards [39]. Calculated degradation levels for samples sintered at different temperatures related to the number of thermal shock cycles is given in Figure 1. Obtained results can be used for material lifetime prediction.

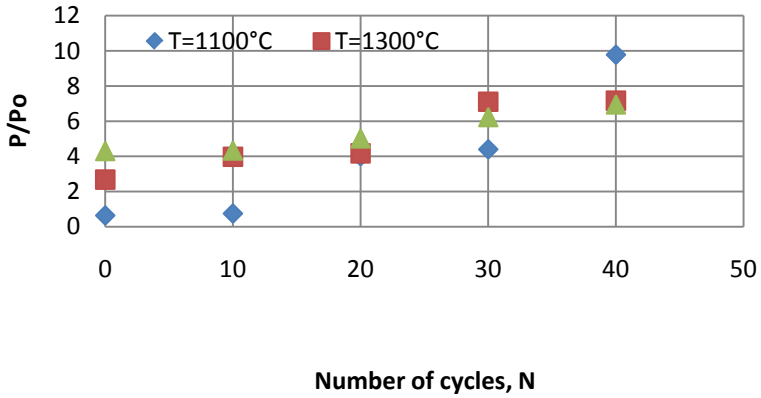

Fig. 2. Surface degradation level during thermal stability testing.

Defects characterization, as well as a comparison of degradation levels for the samples sintered at different temperatures, will be given for samples subjected to 40 cycles of

thermal shock. The behavior of samples sintered at three different temperatures can be estimated by comparison of the number and average and total areas of defects presented in Table II.

Tab. II Defects characterization: number, average and total area of defects.

Characteristic of defects	Sintering temperature(^{o}C)		
	1100	**1300**	**1600**
Number	139	143	120
Average area, cm^2	0.099857	0.006241	0.0567
Total area, cm^2	1.139812	0.90499	0.6917

Quantification of the degradation level can be done using analysis of the samples` surface by number and area of defects and by calculation of the degradation level (P/P_0; where P is the surface area after certain cycles of thermal shock and P_0 is the surface area before thermal shock (initial surface)). Results of degradation levels for the samples sintered at three different temperatures after 40 cycles of thermal shocks are presented in Table II in order to compare their behavior. The presence of a lower number of damages (120) for the sample sintered at 1600°C is observed. The average area (0.0567 cm) and total area of the defects (0.6917) at the same temperature indicate that the formation of defects was slower than for other sintering temperatures. Similar results can be observed after 40 cycles of thermal shock in the case of the samples sintered at 1100 and 1300°C.

3.2 Morphological analysis of defects

Comparison of thermal stability resistance results for samples after 40 cycles based on the morphological descriptors are given in Table III. Chosen descriptors were area, diameter (min, max, and mean), perimeter, roundness, and fractal dimension.

Tab. III Morphological descriptors for different sintering temperatures.

Morphological descriptor, average values	Sintering temperature (^{o}C)		
	1100	1300	1600
Area, cm	1.379956	0.89875	0.686078
Diameter (max),cm	0.158019	0.142323	0.12364
Diameter (min),cm	0.039889	0.054193	0.038274
Diameter (mean),cm	0.08671	0.090595	0.070966
Perimeter,cm	0.754275	0.583513	0.459797
Roundness, cm	7.129077	7.212167	4.729661
Perimeter 2, cm	1.803139	1.548423	1.335936
Perimeter 3,cm	0.832724	0.651374	1.180714
Fractal Dimension	1.236922	1.195622	0.517591

Results summarized in Table III can be very useful for comparing the influence of sintering temperature on morphology of the occurring defects. It can be concluded that due to lower area of degradation and smaller values for diameter and perimeter, higher temperature of sintering provides the slower formation of defects. Results for roundness are expected, as damages are not spherical but in a shape similar to the irregular grains. Based on the results, the best descriptor characteristics (lowest values) were related to the sintering temperature of 1600°C. This analysis can be provided to more thermal shock cycles, and analysis of the mechanism of degradation can be discussed, as it was presented in previous papers [32-37].

3.3 Strength degradation

During thermal stability testing, compressive strength was measured after every five cycles and results are presented in Fig. 3.

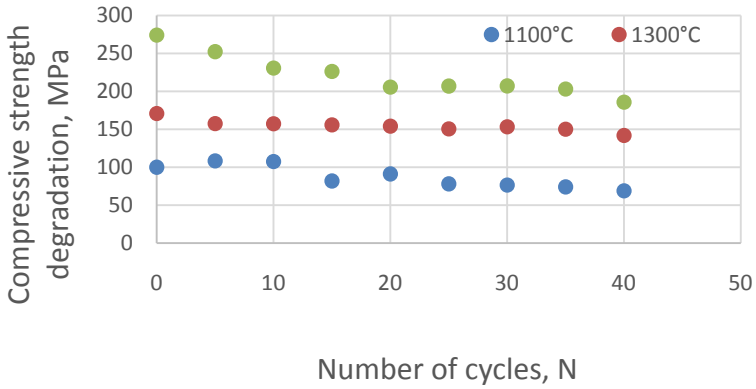

Fig. 3. Compressive strength degradation during thermal stability testing.

Differences for compressive strength degradation suggested that sintering temperature have a great influence on mechanical behavior. Samples sintered at 1100°C exhibited higher values for compressive strength before testing compared to samples sintered at higher temperatures. However, the strength degradation was more rapid compared to other samples. This rapid strength degradation resulted in the fewer number of cycles that the material sintered at 1100°C can withstand. Namely, it is well known that the level of compressive strength before testing is not the only parameter that can point to thermal stability. The strength degradation during testing of samples sintered at 1300 and 1600°C exhibited a lower decrease which indicates higher thermal stability and more cycles that samples can withstand during exposure to the thermal shock.

3.4 Resistance parameters

Fracture R' and damage R''' resistance parameters were calculated based on thermomechanical characteristics and compressive strength degradation during thermal stability testing, for certain numbers of cycles, as well as for all sintered temperatures. Obtained results were presented in Figs 4 and 5.

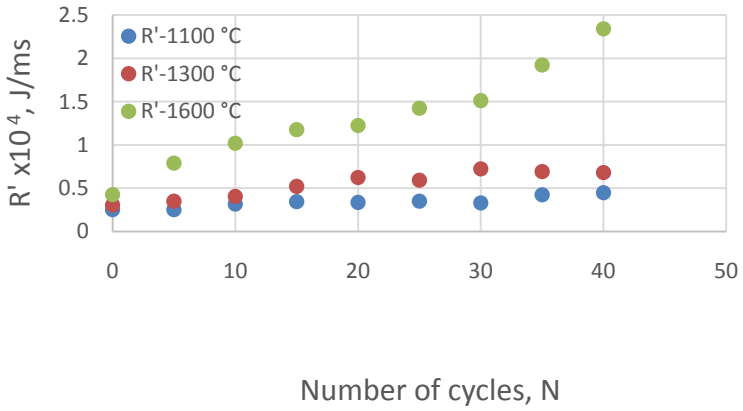

Fig. 4. Fracture resistance parameter R' during thermal stability testing.

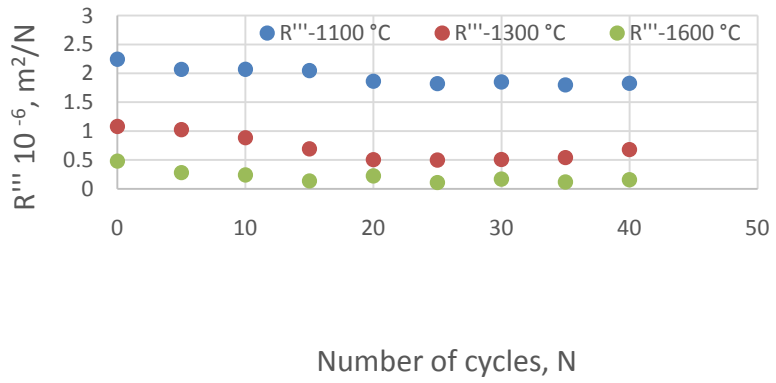

Fig. 5. Damage resistance parameter R‴ during thermal stability testing.

Fracture resistance parameters showed deference for observed sintering temperatures. Samples sintered at 1600°C exhibited the most rapid increase compared to other samples. Samples sintered at lower temperatures indicated a slower increase of R` parameters, but significantly more water quench cycles that the material can withstand according to the standard.

The damage resistance parameter, R''' for samples sintered at all three temperatures are calculated with the aim of describing the behavior of materials with micro pores or micro cracks. Since after 40 cycles of quenching, the test samples had a level of degradation of 9,78 % (1600°C), 7,16 %(1300°C) and 6.95 % (1100°C), that was one of the explanations for it was very important that this parameter was included in the analysis of the behavior of this material at thermal shock.

4. Conclusion

In this paper, different possibilities for thermal stability characterization were discussed, with a detailed analysis of image analysis implementation and resistance parameters. Using image analysis, as a non-destructive method of characterization, is a very useful tool since the results can be related to standard performed testing. Analysis of damage level based on number and area of defects was presented as well as morphological analysis of defects based on different morphological descriptors. Using morphological descriptor analysis, quantification and precisely monitoring of defects formation and growth caused by thermal shock could be achieved.

Using fracture and damage resistance parameters can be useful for comparison different conditions such is sintering temperature in thermal stability experiments. Based on the changes of R parameters values during thermal stability testing, the material selection would be possible when good thermal stability is required.

Acknowledgments

This work was financially supported by the Ministry of Education, Science and Technological Development of the Republic of Serbia (Grant No. 451-03-9/2021-14/200026).

5. References

1. W.D. Kingery, H.K. Bowen, D.R. Uhlmann, Introduction to Ceramics, John Wiley and Sons, New York, 1976.
2. W.D. Kingery, J. Am. Ceram. Soc. 38 (1955) 3-15.
3. P.H. Hasselman, Mater. Sci. Eng. 71 (1985) 251-264.
4. D.P.H. Hasselman, J. Am. Ceram. Soc. 52 (1969) 600-604.
5. D.P.H. Hasselman, J. Am. Ceram. Soc. 53 (1970) 490-495.
6. T.J. Lu, N.A. Fleck, Acta Mater. 46 (1998) 4755-4768.
7. ASTM International, ASTM C1525-04 Standard test method for determination of thermal shock resistance for advanced ceramics by water quenching, 2013.
8. European Standard EN820-3. Determination of resistance to thermal shock by water quenching, 2004.
9. J. Nakayama, J. Am. Ceram. Soc., 48 (11) (1965) 583-587.
10. J. Nakayama, M.Ishizuka, Amer. Cer. Soc. Bull., 45 (7) (1965) 666-669.
11. C.E. Semler, Interceram, 5 (1981) 485-488.
12. F. Aly, C.E. Semler, Am. Ceram. Soc. Bull., 64 (12) (1985) 1555-1558.
13. V. Nakayama, M. Ishizuka, Am. Ceram. Soc. Bull., 45 (7) (1966) 666-669.
14. R.C. Bradt, in: "2nd International Conference on Refractories", Refractories ’87, Vol. 1, Tokyo, 1987, p. 61-68.
15. C. Aksel, P.D. Warren, J. Eur. Ceram, 23 (2003) 301-308.
16. M.R. Izadpanah, A.R.A. Dezfoli, Mater. Sci.–Poland, 27 (1) (2009) 131-140.
17. H. Awaji, S. Min Choi, J. Korean Ceram. Soc., 49 (4) (2012) 385-396.
18. T.D. Volkov Husovic, Z.V. Popovic, Mater. Sci. Technol., 15 (10) (1999) 1216-1219.
19. T. Volkov Husovic, R Jancic, M Cvetkovic, D. Mitrakovic, Z. Popovic, Mater. Lett., 38 (1999) 372-378.
20. T.D. Volkov Husovic, R.M. Jancic, V. Radojevic, Z. Popovic, Key Eng. Mater., 2006-213 (2002) 1701-1703.
21. D. Lewis, J. Am. Ceram. Soc., 63 (11-12) (1980) 713-714.
22. H. Hencke, J.R. Thomas, D.P.H. Hasselman, J. Am. Ceram. Soc.,67, (6) (1984) 393-398.
23. A. Böhm, S. Dudczig, J. Fruhstorfer, A. Mertke, C.G. Aneziris, J. Malzbender, J. Ceram. Sci. Tech., 07 (02) (2016) 155-164.
24. S.S. Manson, R.W. Smith, J. Am. Ceram. Soc., 38 (1) (1955) 18-27.
25. M.R. Izdpanah, A.R.A. Dezfoli, Mater. Sci.–Poland, 27 (1) (2009) 131-140.
26. D.N. Boccaccini, M. Romagnoli, P. Veronesi, M. Cannio, C. Leonelli, G. Pellecani, T. Volkov Husovic, A.R. Boccaccini, Int. J. Appl. Ceram. Technol., 4 (3) (2007) 260-268.
27. Matías R. Gauna, Juan M. Martinez, María S. Conconi, Gustavo Suárez, Nicolás M. Rendtorff, Effect of TiO_2 in Fine Zircon Sintering and Properties, Science of Sintering, 53 (2021) 267-283
28. Juan Manuel Martinez, María F. Hernández, Fernando Booth, Paula V. Lopez, Gustavo Suarez, María S. Conconi, Nicolás M. Rendtorff, Partially Stabilized Zirconia (3Y-ZrO_2) Aluminum Borate ($Al_{18}B_4O_{33}$) Needles Composite Materials by Direct Sintering, Science of Sintering, 53 (2021) 9-18
29. D.N. Boccaccini, M. Cannio,T.D. Volkov–Husović, I. Dlouhy, M. Romagnoli, P. Veronesi, C. Leonelli, J. Eur.Ceram., 28 (2008) 1941-1951.
30. M. Posarac, M. Dimitrijavic, T. Volkov Husovic, J. Majstorovic, B. Matovic, Mater. Des. 30 (8) (2009) 3338-3343.
31. https://www.stressmarq.com/5-free-image-analysis-software-tools-for-microscopy/?v=3e8d115eb4b3
32. Image–Pro Plus, Version 4.0. for Windows, Media Cybernetics, Silver Spring.

33. S. Martinović, J. Majstorović, V. Vidojković, T. Volkov–Husović, Sci. Sinter. 42 (2010) 211-219.
34. S. Martinović, M. Vlahović,T. Boljanac, J. Majstorović, T. Volkov–Husović, Compos. B. Eng, 60 (2014) 400-412.
35. S. Martinovic, M. Dojcinovic, J. Majstorovic, A. Devecerski, B. Matovic, T. Volkov Husovic, J. Eur. Ceram., 30 (2010) 3303-3309.
36. G.F. Vander Voort, Image Analysis, in: Materials Characterization, Ed.: R.E. Whan, ASM International (1986).
37. T.D. Volkov Husovic, R.M. Jancic, D. Mitrakovic, Am. Ceram. Soc. Bull., 84 (10) (2005) 1-5.
38. T.D. Volkov Husovic, J. Majstorovic, M. Cvetkovic, Am. Ceram. Soc. Bull., 85 (3) (2006).
39. T.D. Volkov Husovic, J. Test. Eval., 35 (1) (2006) 1-5.
40. SRPS EN B. D8. 319; Refractories – Methods of physical testing – Determination of the resistance to thermal shock – Water quenching

Сажетак: *Термостабилност спада у један од параметара који имају веома важну улогу у избору оптималног ватросталног материјала. Различите методе карактеризације су биле развијене у сврху што бољег дефинисања термостабилности, укључујући недеструктивне методе. Анализа слике је веома добар метод карактеризације различитих материјала и структура, као и праћења промена и насталих дефеката изазваних раличитим утицајним факторима. У оквиру овог рада примена анализе слике ће бити приказана у циљу праћења понашања одбраних узорака током испитивања термпстабилности. Разичити параметри, као што су R параметри , степен оштећења, , као морфолошки дескриптори (површина, периметер, пречник, заобљеност) применом анализе слике ће бити обрађени у оквиру овог рада.*
Кључне речи*: Термостабилност; ватростални материјал; R параметри; анализа слике.*